EPJ manuscript No.
(will be inserted by the editor)

Optical absorption in boron clusters B_6 and B_6^+: A first principles configuration interaction approach

Ravindra Shinde and Alok Shukla

Department of Physics, Indian Institute of Technology Bombay, Mumbai, Maharashtra, India 400076. e-mail: ravindra.shinde@iitb.ac.in, shukla@phy.iitb.ac.in

Received: date / Revised version: date

Abstract. The linear optical absorption spectra in neutral boron cluster B_6 and cationic B_6^+ are calculated using a first principles correlated electron approach. The geometries of several low-lying isomers of these clusters were optimized at the coupled-cluster singles doubles (CCSD) level of theory. With these optimized ground-state geometries, excited states of different isomers were computed using the singles configuration-interaction (SCI) approach. The many body wavefunctions of various excited states have been analysed and the nature of optical excitation involved are found to be of collective, plasmonic type.

Key words. boron, optical, absorption, configuration, interaction, correlation, SCI

arXiv:1208.6536v1 [physics.atm-clus] 31 Aug 2012

1 Introduction

The cluster science is now a fast emerging field with novel properties and tremendous potential for applications. A cluster of atoms, or molecules can have few atoms to thousands of atoms in it, with various structural forms, such as spheres, tubes, planar structures *etc.* Most of the time, the properties exhibited by clusters are completely different than their bulk counterpart [1,2]. Boron, in particular, is as interesting as carbon, because of its short covalent radius and ability to form any structure due to catenation. Boron also exhibits structures like nanotubes, fullerenes, planar sheets etc. Some of the structures of boron have been studied in the context of hydrogen storage [3]. Both σ and π aromaticity is observed in many planar boron clusters. Some planar boron structures are also found to be analogous to hydrocarbons [4]. A circular B_{19}^- cluster, with a unit of B_6 wheel in the center behaves as a Wankel motor, *i.e.* the inner B_6 wheel rotating opposite to the outer B_{13} ring [5,6]. The all-boron clusters are promising candidates as inorganic ligands [7,8].

There have been various experimental and theoretical investigations of bare boron clusters. Electronic structures of boron quasi-planar structures, tubes, wheels and rings were studied experimentally using photo-emission spectroscopy by Wang and co-workers [4,9,10,11]. They also gave a density functional theory (DFT) based explanation of their electronic structure. Alexandrova *et. al.* explored the structural and electronic properties and chemical bonding in B_6^- and B_6 using anion photoelectron spectroscopy and *ab initio* calculations [12]. La Placa, Roland and Wynne studied abundance spectrum of boron clusters generated using laser ablation technique [13]. Ionic boron clusters were experimentally studied by Hanley, Whitten and Anderson [14]. They studied the fragmentation of bigger clusters into smaller ones by studying the collision-induced dissociation of boron clusters. Boustani, on the other hand, gave a theoretical description of electronic structures of small bare boron clusters using configuration interaction method, although with a relatively small Gaussian basis set [15]. Recently a DFT based study of bare boron clusters was done by Atiş, Özdogan and Güvenç [16]. As far as optical properties of boron clusters are concerned, there are very few reports available. Marques and Botti studied the optical absorption spectra of B_{20}, B_{38}, B_{44}, B_{80} and B_{92} using time-dependent DFT [17]. To the best of our knowledge, no other experimental results are available on the optical absorption of boron clusters.

Our group has recently studied the optical absorption in boron clusters B_n (n=2 – 5) using a large-scale multi-reference configuration interaction method [18]. Since this method is quite extensive and scales as N^6, where N is the number of orbitals used in the calculations, it cannot be applied for large clusters, or clusters with no symmetry. However good insights can be achieved with relatively less extensive method known as singles configuration interaction (SCI), containing only one electron excitations from the Hartree-Fock ground state. This method has been extensively used for the study of the excited states and optical absorption in various other systems [19,20,21,22,23,24]. Since optical absorption spectra is very sensitive to the structural geometry, the optical absorption spectroscopy along with the extensive calculations of optical absorption spectra, can be used to distinguish between distinct isomers of a cluster. In this report, we present an extensive calculations of the linear optical absorption spectrum of low-lying isomers of B_6 and B_6^+ clusters with different

structures. This study along with experimental absorption spectra can lead to identification of these distinct isomers. Also, in the interpretation of the measured spectra, the theoretical insight of the excited states of clusters play an important role [25].

The remainder of this paper is organised as follows. Next section describes the theoretical and computational details of the work, followed by section 3, in which results are presented and discussed. In the last section we present our conclusions, and explore the scope for future work. Detailed information regarding the excited states contributing to the optical absorption is presented in the appendix.

2 Theoretical and Computational Details

Different possible arrangements and orientations of atoms of the B_6 cluster (both neutral and cationic) were randomly selected for the initial configurational search of geometries of isomers. For a given spin multiplicity, the geometry optimization was done at a correlated level, i.e. at singles doubles coupled cluster (CCSD) level with 6-311G(d,p) basis set as implemented in `Gaussian 09` [26]. Since neutral cluster can have singlet or higher spin multiplicity, the optimization was repeated for different spin configurations to get the lowest energy isomer. Similarly for cationic clusters with odd number of electrons, spin multiplicities of 2 and 4 were considered in the optimization. In total, we have obtained 11 neutral B_6 and 8 cationic B_6^+ low-lying isomers. These optimized geometries of neutral B_6 cluster, as shown in Fig. 1, are found to be in good agreement with other available reports. Figure 3 shows the corresponding geometries of cationic B_6^+ cluster. The unique bond lengths, point group symmetry and the electronic ground states are given in respective sub-figures.

For finite systems, such as clusters or quantum dots, the ratio $\frac{a}{\lambda} \ll 1$, where a is system size and λ is incident wavelength of light. In this case, the optical absorption cross section of the system corresponding to linear absorption can be computed within the electric dipole approximation,

$$\sigma_n(\omega) = 4\pi\alpha \sum_i \frac{\omega_{in}|\langle i|\hat{e}.\bar{\boldsymbol{r}}|n\rangle|^2\gamma}{(\omega_{in}-\omega)^2+\gamma^2} \qquad (1)$$

where, α is fine structure constant, ω_{in} is frequency corresponding to energy difference of final state $|i\rangle$ and initial state $|n\rangle$. $\bar{\boldsymbol{r}}$ denotes position vector and γ is linewidth of absorption.

The excited state energies of isomers are obtained using the *ab initio* SCI approach. In this method, different configurations are constructed by replacing one of the occupied molecular orbitals in the Hartree-Fock ground state by a virtual orbital. Excited states of the system will have a linear combination of all such substituted configurations, with corresponding variational coefficients. The energies of the excited states will then be obtained by diagonalizing the Hamiltonian in this configurational space [27]. The dipole matrix elements are calculated using the ground state and the excited state wavefunctions. This is subsequently used for calculating the optical absorption cross section assuming Lorentzian lineshape, with some artificial finite linewidth (*cf.* Eqn. 1). The contribution of wavefunction of the excited states to the absorption peaks gives an insight into the nature of optical excitation.

In one of the earlier reports published elsewhere[18], we have extensively studied the dependence of basis sets, freezing of $1s^2$ chemical core and energy cutoff on virtual orbitals on the computed photoabsorption spectra of neutral boron clusters [18]. We have shown that the optical absorption spectra of small boron clusters do not change even if we freeze the chemical core of boron atoms. Also, a careful investigation was done for obtaining the energy cutoff of virtual orbitals to be included in the active space. Hence, in the present calculations, we have taken augmented correlation consistent polarized valence double zeta Gaussian basis set [28,29]. We also froze the chemical core, and kept only those virtual orbitals with energies of 1 Hartree or less.

3 Results and Discussion

In this section, we discuss the structure and energetics of various isomers of neutral and cationic B_6 cluster, followed by discussion of results of computed absorption spectra and nature of photo-excitations.

In the many-particle wavefunction analysis of excited states contributing to the various peaks , we have used following convention. For doublet systems H_1 denotes the singly occupied molecular orbital. For triplet systems, two singly occupied molecular orbitals are denoted by H_1 and H_2, while H and L stands for highest occupied molecular orbital and lowest unoccupied molecular orbital respectively. For quartets, the third singly occupied molecular orbital is denoted by H_3.

3.1 B_6

We have found a total of 11 isomers of neutral B_6 cluster with stable geometries as shown in the Fig. 1 [30]. The relative standings in energy are presented in the Table 1, along with point group symmetries and electronic states.

Table 1. Point group, electronic state and total energies of different isomers of B_6 cluster.

Sr. no.	Isomer	Point group	Elect. State	Total Energy (Ha)
1	Planar ring (triplet)	C_{2h}	^3A_u	-147.795051
2	Incomplete wheel	C_{2v}	$^3B_1$	-147.774166
3	Bulged wheel	C_{5v}	$^1A_1$	-147.764477
4	Planar ring (singlet)	C_s	$^1A^{'}$	-147.720277
5	Octahedron	O_h	$^3A_{1g}$	-147.678302
6	Threaded tetramer	C_1	^3A	-147.676776
7	Threaded trimer	C_{2v}	$^3B_1$	-147.667709
8	Twisted trimers	C_1	^1A	-147.645847
9	Planar trimers	D_{2h}	^1A_g	-147.645522
10	Convex bowl	C_1	^1A	-147.612607
11	Linear	$D_{\infty h}$	$^1\Sigma_g$	-147.449013

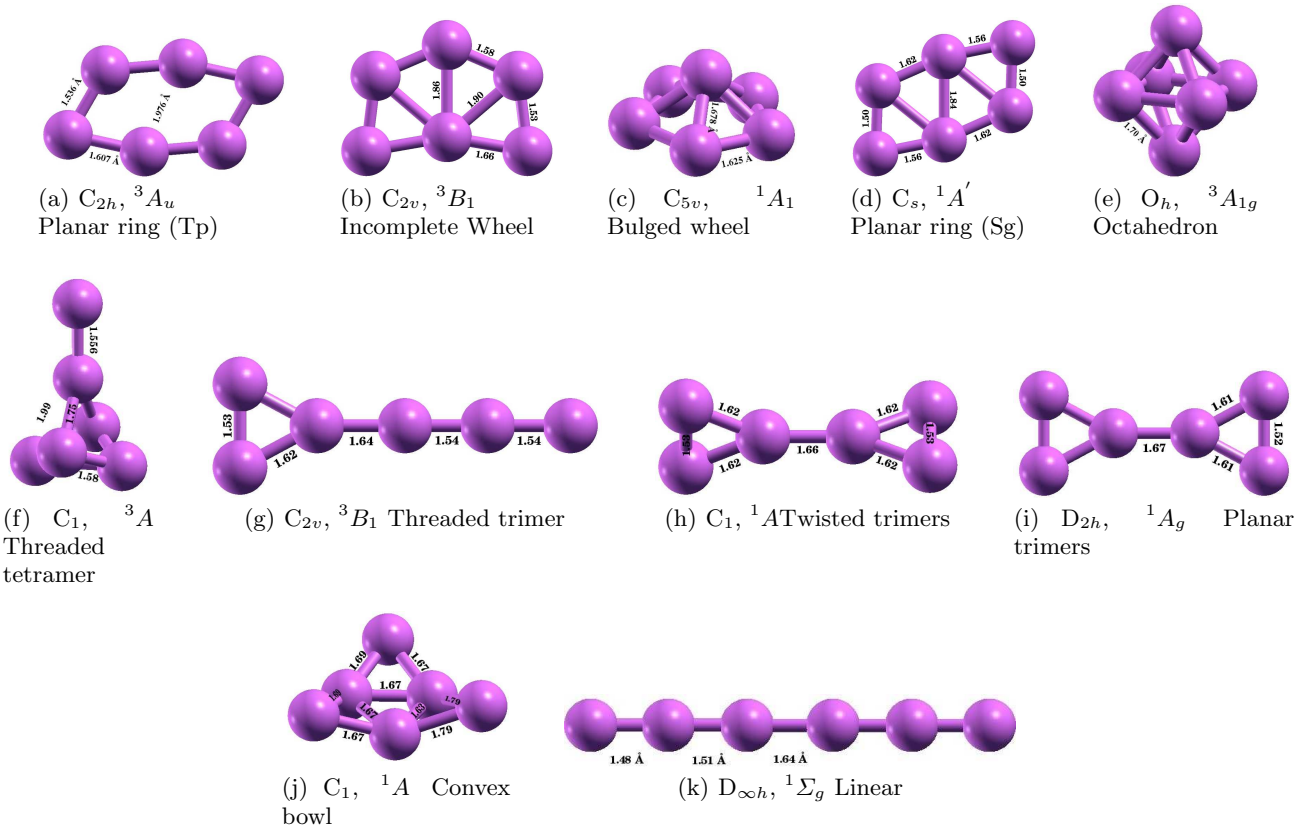

(a) C_{2h}, ^3A_u Planar ring (Tp)
(b) C_{2v}, $^3B_1$ Incomplete Wheel
(c) C_{5v}, $^1A_1$ Bulged wheel
(d) C_s, $^1A^{'}$ Planar ring (Sg)
(e) O_h, $^3A_{1g}$ Octahedron
(f) C_1, ^3A Threaded tetramer
(g) C_{2v}, $^3B_1$ Threaded trimer
(h) C_1, ^1ATwisted trimers
(i) D_{2h}, ^1A_g Planar trimers
(j) C_1, ^1A Convex bowl
(k) $D_{\infty h}$, $^1\Sigma_g$ Linear

Fig. 1. (Color online) Geometry optimized ground state structures of different isomers of neutral B_6 clusters, along with the point group symmetries obtained at the CCSD level.

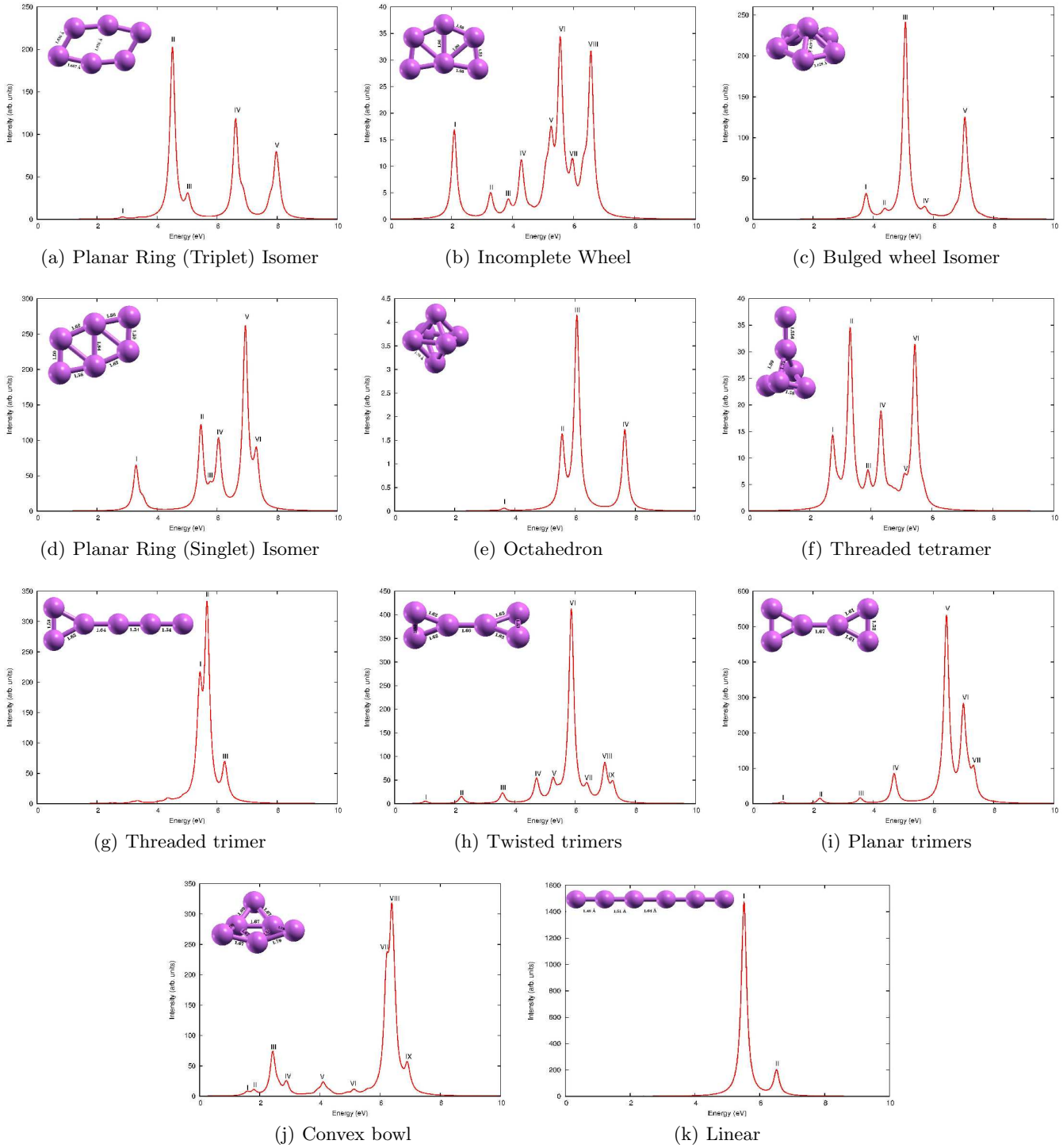

(a) Planar Ring (Triplet) Isomer (b) Incomplete Wheel (c) Bulged wheel Isomer

(d) Planar Ring (Singlet) Isomer (e) Octahedron (f) Threaded tetramer

(g) Threaded trimer (h) Twisted trimers (i) Planar trimers

(j) Convex bowl (k) Linear

Fig. 2. (Color online) The linear optical absorption spectrum of B_6, calculated using the SCI approach. The many-body wavefunctions of excited stated corresponding to the peaks labeled are given in the Appendices A.1–A.11. For plotting the spectrum, a uniform linewidth of 0.1 eV was assumed.

The most stable isomer of B_6 cluster has ring-like planar structure, with C_{2h} point group symmetry. Although B_6 has an even number of electrons, the electronic ground state of this isomer is a triplet – an open shell system. The equilibrium geometry obtained in our calculation is in good agreement with the recently reported values [12,16,31,32]. The optical absorption spectrum calculated using the SCI approach is as shown in the Fig. 2(a). It is mainly characterized by feeble absortion in the visible range, but much stronger absorption at higher energies. The many particle wave-functions of excited states contributing to various peaks are presented in Table A.1. The first absorption peak at 2.84 eV with very low intensity is characterized by $H-3 \rightarrow H_2$ and $H-1 \rightarrow H_1$ transitions. Due to planar nature of the isomer, we can classify the absorption into two categories: (a) those with polarization along the direction of the plane and (b) polarization perpendicular to the plane. In this case, it is seen that, in most of the cases, the absorption is due to polarizations along the plane of the isomer. Also, instead of being dominated by single configurations, the wavefunctions of the excited states contributing to all the peaks exhibit strong configuration mixing. This is an indicator of plasmonic nature of the optical excitations [33].

The second low lying isomer of B_6 is another planar structure resembing an incomplete wheel, *i.e.* one outer atom removed from B_7 wheel cluster. This isomer is also a triplet system with C_{2v} symmetry, lying 0.56 eV above the global minimum structure. The optimized geometry is in good agreement with the other previously available reports [31,34]. This is one of the isomers showing optical absorption at lower energies (*cf.* Fig. 2(b)). The many particle wave-functions of excited states contributing to various peaks are presented in Table A.2. An intense peak at around 2.1 eV is seen in this isomer, characterized by $H_1 \rightarrow L+1$ and $H_2 \rightarrow L$ transitions.

A wheel kind of structure, with its center slightly bulged out, is found to be the next stable isomer of B_6. A singlet system with C_{5v} point group symmetry, lies just 0.83 eV above in energy as compared to the most stable isomer. The pentagonal base has bond length of 1.625 Å and the vertex atom is 1.678 Å apart from the corners of the pentagon. Other reported values for those bond lengths are 1.61 Å, 1.66 Å [16,34] and 1.61 Å, 1.659 Å [12,31] respectively. The optical absorption spectrum is presented in Fig. 2(c). The many-particle wave functions of excited states contributing to various peaks are presented in Table A.3. The onset of the spectrum occurs near 3.76 eV, with polarization in the plane of the pentagonal base, characterized by excitations $H-1 \rightarrow L+6$ and $H \rightarrow L+6$ with equal contribution.

A planar ring like structure, resembling the global minimum one; however, with singlet state and C_s symmetry, is the next low lying isomer of B_6 cluster. The optimized geometry is in good agreement with Ref. [34]. The absorption spectrum is presented in Fig. 2(d) and corresponding many-particle wavefunctions of various excited states are presented in Table A.4. The absorption starts at the end of visible range, characterized by $H-1 \rightarrow L$ and $H \rightarrow L+23$.

An octahedron structure with O_h point group symmetry is the next stable isomer of neutral B_6. Each side of the octahedron is found to be 1.7 Å as compared to the 1.68 Å reported by [16] and [34]. The many-particle wave functions of the excited states correponding to various peaks (*cf.* Fig. 2(e)) are presented in Table A.5. A very feeble absorption at 3.6 eV opens the spectrum, mainly characterized by excitations $H-1 \rightarrow L$ and $H-1 \rightarrow L+1$ with equal contribution.

Next isomer is previously unreported, with structure of a saddle threaded with dimer from top. It lies just 0.04 eV above the previous octahedron isomer. However the optical absorption spectrum (*cf.* Fig. 2(f)) is completely different. A narrow energy range hosts all the peaks. The onset of spectrum occurs near 2.7 eV, with major contribution from $H-1 \rightarrow H_2$ and $H_1 \rightarrow L+9$ (*cf.* Table A.6).

An isosceles triangle connected to a linear chain of boron atoms forms the next isomer. This structure with C_{2v} symmetry and a triplet electronic state have been reported in [34], which is in close agreement with our results. The optical absorption spectrum (*cf.* Fig. 2(g)) has distinctive closly lying peaks at 5.42 eV and 5.66 eV. The many-particle wavefunctions of excited states corresponding to various peaks are presented in Table A.7. Configurations $H-3 \rightarrow L$ and $H-1 \rightarrow L+1$ contribute predominently to those closly lying peaks respectively.

A structure with two out of plane isosceles triangles joined together is found to be one of the isomers. The geometry has isosceles triangle with lengths 1.62 Å, 1.62 Å and 1.53 Å, while two such triangles are joined by a bond of length 1.66 Å. The respective numbers reported by Ref. [34] are 1.60 Å, 1.60 Å, 1.50 Å and 1.647 Å respectively. The optical absorption spectrum contains many low intensity peaks except for strongest one at 5.87 eV, as presented in Fig. 2(h). The onset of the spectrum occurs at 1 eV – a peak equally dominated by $H \rightarrow L$ and $H-1 \rightarrow L$ (*cf.* Table A.8).

An almost degenerate structure forms the next isomer, lying just 0.009 eV above the previous isomer. Contrary to the previous one, this geometry is completely planar and is a triplet system, with C_{2v} point group symmetry. Probably because of such a strong near-degeneracy, this isomer has not been reported in the literature before. The many-particle wave functions of the excited states corresponding to various peaks (*cf.* Fig. 2(i)) are presented in Table A.9. The spectrum opens with a very feeble peak $H \rightarrow L$ and $H-1 \rightarrow L+1$ as dominant contributions to the excited state wavefunction.

Convex bowl shaped isomer and a perfect linear chain are found very high in energy, ruling out their existence at room temperature. The optical spectra are presented in Figs. 2(j) and 2(k) respectively. The corresponding many-particle wavefunctions of excited states of various peaks are presented in Table A.10 and A.11. The onset of absorption spectrum of convex bowl isomer occurs at 1.58 eV with $H-1 \rightarrow L+1$ as the most dominant configuration. The bulk of the oscillator strength of the spectrum of linear isomer is carried by $H-1 \rightarrow L+3$ and $H \rightarrow L+2$ having equal contributions.

3.2 B_6^+

We have found a total of 8 isomers of cationic (B_6^+) cluster with stable geometries as shown in the Fig. 3. The relative standings in energy are presented in the Table 2, along with point group symmetries and electronic states.

Table 2. Point group, electronic state and total energies of different isomers of B_6^+ cluster.

Sr. no.	Isomer	Point group	Elect. State	Total Energy (Ha)
1	Planar ring (I)	C_s	$^2A''$	-147.492831
2	Bulged wheel	C_1	^2A	-147.491994
3	Planar ring (II)	D_{2h}	^2A_g	-147.480796
4	Incomplete wheel	C_{2v}	$^4A_2$	-147.454234
5	Threaded trimer	C_{2v}	$^4A_2$	-147.429627
6	Tetra. bipyramid	D_{4h}	$^2B_{1g}$	-147.413145
7	Linear	$D_{\infty h}$	$^4\Sigma_u$	-147.392263
8	Planar trimers	D_{2h}	$^2B_{2g}$	-147.358494

Cationic clusters show activity in the visible range, contrary to their neutral counterpart. Also, in most of the cases the geometry of the neutral isomer is retained, reflected in the fact that some peaks show up in the optical absorption spectra at the same energies as those in the neutral cluster.

The most stable isomer of B_6^+ cluster is a planar ring-type of structure, with C_s point group symmetry. This is in contrast to the other reported geometries which have D_{2h} symmetry [31,32,34]. A slight difference in the orientation makes it less symmetric. However, the bonds lengths obtained are in good agreement with those with D_{2h} symmetric geometry cited above. The optical absorption spectrum calculated using SCI approach is as shown in the Fig. 4(a) and corresponding many particle wavefunctions of excited states contributing to the various peaks are presented in Table A.12. Similar to the neutral counterpart, this isomer also has very feeble absorption in the visible range, with polarization perpendicular to the plane of the isomer. The dominant contribution to the peak at 0.63 eV comes from $H_1 \rightarrow L$ and $H-2 \rightarrow L+16$. The spectrum is slightly red-shifted with respect to the neutral counterpart.

Bulged wheel structure is the next low lying isomer of B_6^+ with just 0.023 eV above the global minimum. However, as compared to the neutral one, this geometry has C_1 symmetry due to the significant bond length reordering. Our results are consistent with the results of Refs. [31,34]. The optical absorption spectrum is presented in Fig. 4(b). The many-particle wave functions of excited states contributing to various peaks are presented in Table A.13. The spectrum is distinctly different with bulk of the oscillator strength carried by peaks at 6 eV. The onset of spectrum occurs at 1.67 eV dominated by $H-2 \rightarrow H_1$ and $H_1 \rightarrow L+3$ configurations.

Another ring-like structure with D_{2h} symmetry and doublet multiplicity lies next in the energy order. The six faced benzene type structure has 1.66 Å and 1.53 Å as unique bond lengths, which are somewhat larger than those reported in the literature [31,34].The optical absorption spectrum is presented in Fig. 4(c). The many-particle wave functions of excited states contributing to various peaks are presented in Table A.14. All absorption peaks are due to the polarization along the plane of the isomer.

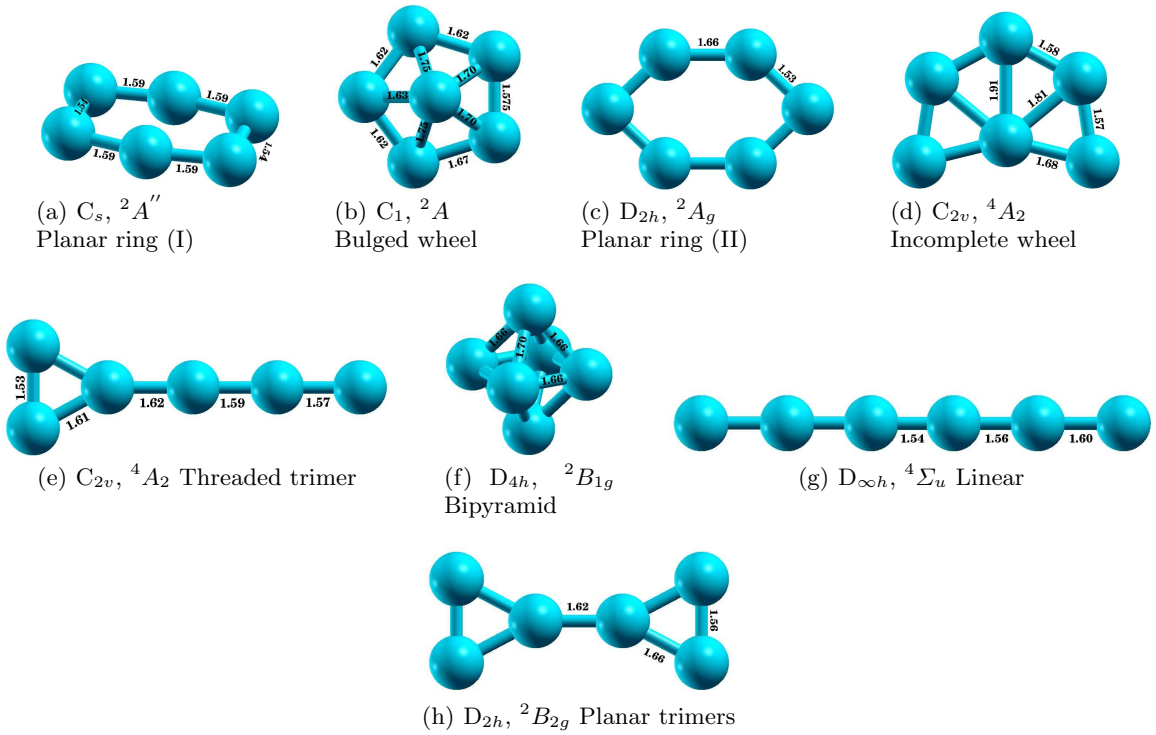

(a) C_s, $^2A''$ Planar ring (I)
(b) C_1, ^2A Bulged wheel
(c) D_{2h}, ^2A_g Planar ring (II)
(d) C_{2v}, $^4A_2$ Incomplete wheel
(e) C_{2v}, $^4A_2$ Threaded trimer
(f) D_{4h}, $^2B_{1g}$ Bipyramid
(g) $D_{\infty h}$, $^4\Sigma_u$ Linear
(h) D_{2h}, $^2B_{2g}$ Planar trimers

Fig. 3. (Color online) Geometry optimized ground state structures of different isomers of cationic B_6^+ clusters, along with the point group symmetries obtained at the CCSD level.

The onset of spectrum occurs at 1.2 eV with a very feeble peak with dominant contributions from $H-1 \rightarrow L$ and $H-2 \rightarrow H_1$.

Next low lying isomer is a planar incomplete wheel structure with C_{2v} point group symmetry and quartet multiplicity. This is consistent with results of Ref. [34]. The optical absorption (*cf.* Fig. 4(d)) starts at 2.94 eV, with polarization transverse to the plane of the isomer. The many particle wave-functions of excited states contributing to various peaks are presented in Table A.15. The configurations contributing to the first peak are $H_1 \rightarrow L+1$ and $H_2 \rightarrow L$, where H_1 and H_2 are singly occupied molecular orbitals of the quartet system.

Another isomer with the same point group symmetry and multiplicity as that of the previous one, but having a geometry of linear chain with an isosceles triangle at the end, is the next low lying isomer of cationic B_6^+. Our results about geometry are in good agreement with the Ref. [34]. The optical absorption spectrum (*cf.* Fig. 4(e)) has very few peaks. The onset of spectrum occurs at 3.2 eV, with polarization along the plane of the isomer, and has dominant contribution from $H-3 \rightarrow H_3$ and $H-3 \rightarrow L$ (*cf.* Table A.16).

Tetragonal bipyramid forms the next stable isomer of cationic B_6^+, with D_{4h} point group symmetry and doublet multiplicity. This is in good agreement with the geometries reported in Refs. [31] and [34]. The optical absorption spectrum (*cf.* Fig. 4(f)) has peaks in the visible range at 1.58 eV and 1.97 eV, with dominant contribution from $H_1 \rightarrow L+2$ and $H-1 \rightarrow L+2$ respectively (*cf.* Table A.17).

Two more structures were found stable *i.e.* (a) a planar structure with two trimers joined together and, (b) a linear one. These isomers are much above the global minimum energy, it rules out their room temperature existence. In the linear isomer the absorption begins with a small peak at 0.93 eV, with dominant contribution from $H-3 \rightarrow H_3$ and $H-1 \rightarrow L$ configurations. In case of planar trimers structure, the spectrum seems to be red shifted as compared to the neutral one. The first peak is found at 0.77 eV with $H-2 \rightarrow H_1$ and $H_1 \rightarrow L+4$ as dominant contribution to the wavefunction of the excited state.

4 Conclusion and Outlook

A large number of randomly selected initial structures of neutral B_6 and cationic B_6^+ clusters are taken into consideration for locating the global and local minimas on the potential energy curves. A careful geometry optimization is done for all those structures at a correlated level. The optical absorption spectra of different low-lying isomers of both neutral and cationic isomers are reported here. A singles configuration interaction approach was used to compute excited state energies and the absorption spectra of various clusters. Spectra of cationic clusters appear slightly red-shifted with respect to the neutral one. Different isomers exhibit distinct optical response, even though

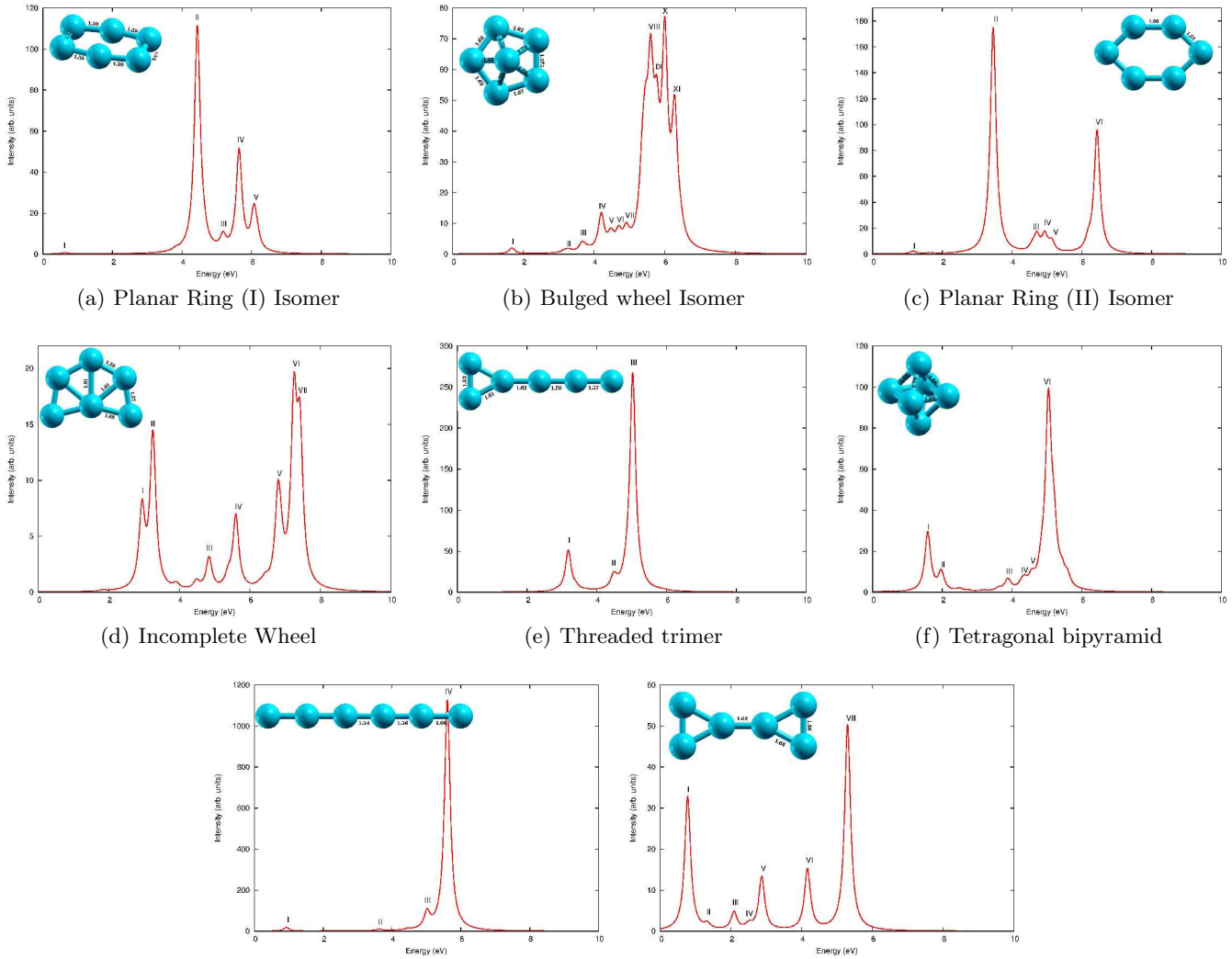

(a) Planar Ring (I) Isomer (b) Bulged wheel Isomer (c) Planar Ring (II) Isomer

(d) Incomplete Wheel (e) Threaded trimer (f) Tetragonal bipyramid

(g) Linear (h) planar bingo

Fig. 4. (Color online) The linear optical absorption spectrum of B_6^+, calculated using the SCI approach. The many-body wavefunctions of excited stated corresponding to the peaks labeled are given in the Appendices A.12– A.19. For plotting the spectrum, a uniform linewidth of 0.1 eV was assumed.

they are isoelectronic and many of them are almost degenerate. This signals a strong-structure property relationship, which can be exploited for experimental identification of these isomers; something which is not possible with the conventional mass spectrometry. A strong mixture of configurations in the many-body wave functions of various excited states are observed, indicating the plasmonic nature of the photoexcited states [33].

Since aluminum also has the same number of valence electrons, it will be interesting to compute its optical absorption spectra, and compare them with those of boron cluster with the help of many-body wavefunctional analysis. The results of such calculations done by us will be communicated in near future [35].

The author would like to acknowledge the Council of Scientific and Industrial Research (CSIR), India, for their financial support (SRF award No. 09/087/(0600)2010-EMR-I and travel grant no. TG/6939/12–HRD).

A Excited State CI Wavefunctions, Energies and Oscillator Strengths

In the following tables, we have given the excitation energies (with respect to the ground state), and the many body wavefunctions of the excited states, corresponding to the peaks in the photoabsorption spectra of various isomers listed in Fig. 1 and Fig. 3 , along with the oscillator strength f_{12} of the transitions,

$$f_{12} = \frac{2}{3}\frac{m_e}{\hbar^2}(E_2 - E_1)\sum_i |\langle m|d_i|G\rangle|^2 \qquad (2)$$

where, $|m\rangle$ denotes the excited state in question, $|G\rangle$, the ground state, and d_i is the i-th Cartesian component of the electric dipole operator. The single excitations are with respect to the reference state as given in respective tables.

Table A.1. Excitation energies, E, and many-particle wave functions of excited states corresponding to the peaks in the linear absorption spectrum of B_6 – planar ring (triplet) isomer (*cf.* Fig. 2(a)). The subscript $\parallel$ in the peak number denotes the absorption due to light polarized in the plane of isomer. In the wave function, the bracketed numbers are the CI coefficients of a given electronic configuration. Symbols H_1,H_2 denote SOMOs discussed earlier, and H, and L, denote HOMO and LUMO orbitals respectively. Note that, the reference state does not correspond to any peak, instead it represents the reference state from which singles excitations are occuring.

Peak	E (eV)	f_{12}	Wave Function
Reference			$\|H_1^1; H_2^1\rangle$
$I_\parallel$	2.84	0.0187	$\|H-3 \rightarrow H_2\rangle(0.7353)$ $\|H-1 \rightarrow H_1\rangle(0.5873)$
$II_\parallel$	4.51	1.7647	$\|H-1 \rightarrow H_1\rangle(0.7214)$ $\|H-3 \rightarrow H_2\rangle(0.4417)$
$III_\parallel$	5.03	0.2023	$\|H-3 \rightarrow L\rangle(0.5919)$ $\|H-1 \rightarrow L+8\rangle(0.5137)$
$IV_\parallel$	6.62	0.9942	$\|H-1 \rightarrow L+8\rangle(0.5440)$ $\|H-1 \rightarrow L+3\rangle(0.4900)$
$V_\parallel$	7.96	0.5799	$\|H-1 \rightarrow L+3\rangle(0.6800)$ $\|H-1 \rightarrow L+8\rangle(0.5298)$

Table A.2. Excitation energies, E, and many-particle wave functions of excited states corresponding to the peaks in the linear absorption spectrum of B_6 – incomplete wheel isomer (*cf.* Fig. 2(b)). The subscripts $\parallel$ and $\perp$, in the peak number denote the absorption due to light polarized in, and perpendicular to the plane of wheel base, respectively. The rest of the information is the same as given in the caption for Table A.1.

Peak	E (eV)	f_{12}	Wave Function
Reference			$\|H_1^1; H_2^1\rangle$
$I_\parallel$	2.09	0.1460	$\|H_1 \rightarrow L+1\rangle(0.8102)$ $\|H_2 \rightarrow L\rangle(0.2871)$
$II_\parallel$	3.28	0.0406	$\|H_2 \rightarrow L\rangle(0.9011)$ $\|H-1 \rightarrow H_1\rangle(0.2359)$
$III_\perp$	3.86	0.0247	$\|H-3 \rightarrow H_2\rangle(0.9301)$ $\|H-3 \rightarrow L+27\rangle(0.2154)$
$IV_\parallel$	4.28	0.0849	$\|H-2 \rightarrow H_2\rangle(0.7926)$ $\|H-1 \rightarrow H_1\rangle(0.3875)$
$V_\parallel$	5.26	0.1008	$\|H-5 \rightarrow H_1\rangle(0.4241)$ $\|H-1 \rightarrow H_1\rangle(0.4168)$
$VI_\parallel$	5.56	0.2772	$\|H_1 \rightarrow L+16\rangle(0.5724)$ $\|H_1 \rightarrow L+5\rangle(0.3863)$
$VII_\parallel$	5.96	0.0677	$\|H_1 \rightarrow L+18\rangle(0.5153)$ $\|H_1 \rightarrow L+8\rangle(0.3795)$
$VIII_\parallel$	6.57	0.1286	$\|H-1 \rightarrow L\rangle(0.5208)$ $\|H-5 \rightarrow L\rangle(0.5092)$

Table A.3. Excitation energies, E, and many-particle wave functions of excited states corresponding to the peaks in the linear absorption spectrum of B_6 – bulged wheel isomer (*cf.* Fig. 2(c)). The subscripts $\parallel$ and $\perp$, in the peak number denote the absorption due to light polarized in, and perpendicular to the plane of wheel base, respectively. In the wave function, the bracketed numbers are the CI coefficients of a given electronic configuration. Symbols H and L denote HOMO and LUMO orbitals respectively. Excitations are with respect to Hartree Fock reference state.

Peak	E (eV)	f_{12}	Wave Function
$I_\parallel$	3.76	0.2625	$\|H-1\rightarrow L+6\rangle(0.5622)$ $\|H\rightarrow L+6\rangle(0.5622)$ $\|H-1\rightarrow L+2\rangle(0.4459)$ $\|H\rightarrow L+2\rangle(0.4459)$
$II_\parallel$	4.38	0.0657	$\|H-1\rightarrow L+3\rangle(0.4998)$ $\|H\rightarrow L+3\rangle(0.4998)$ $\|H-1\rightarrow L+4\rangle(0.4981)$ $\|H\rightarrow L+4\rangle(0.4981)$
$III_\parallel$	5.07	2.1039	$\|H-2\rightarrow L+1\rangle(0.7653)$ $\|H-2\rightarrow L\rangle(0.7653)$ $\|H-2\rightarrow L+8\rangle(0.2857)$ $\|H-2\rightarrow L+7\rangle(0.2857)$
$IV_\perp$	5.71	0.0810	$\|H-2\rightarrow L+6\rangle(0.6266)$ $\|H-2\rightarrow L+2\rangle(0.5564)$
$V_\parallel$	7.05	1.0550	$\|H\rightarrow L+5\rangle(0.7645)$ $\|H-1\rightarrow L+5\rangle(0.7645)$ $\|H\rightarrow L+6\rangle(0.4763)$ $\|H-1\rightarrow L+6\rangle(0.4763)$

Table A.4. Excitation energies, E, and many-particle wave functions of excited states corresponding to the peaks in the linear absorption spectrum of B_6 – planar ring (singlet) isomer (*cf.* Fig. 2(d)). The subscripts $\parallel$ and $\perp$, in the peak number denote the absorption due to light polarized in, and perpendicular to the plane of the isomer, respectively. The rest of the information is the same as given in the caption for Table A.3.

Peak	E (eV)	f_{12}	Wave Function
$I_\parallel$	3.29	0.5397	$\|H-1\rightarrow L\rangle(0.9174)$ $\|H\rightarrow L+23\rangle(0.2504)$
$II_\parallel$	5.46	1.0153	$\|H\rightarrow L+7\rangle(0.4991)$ $\|H\rightarrow L+23\rangle(0.4093)$
$III_\parallel$	5.77	0.1380	$\|H-1\rightarrow L+2\rangle(0.5479)$ $\|H-1\rightarrow L+8\rangle(0.5181)$
$IV_{\parallel,\perp}$	6.04	0.8199	$\|H\rightarrow L+7\rangle(0.7472)$ $\|H\rightarrow L+12\rangle(0.3140)$
$V_\parallel$	6.93	2.2212	$\|H\rightarrow L+16\rangle(0.4623)$ $\|H\rightarrow L+12\rangle(0.4600)$
$VI_\parallel$	7.31	0.6003	$\|H\rightarrow L+16\rangle(0.6363)$ $\|H\rightarrow L+12\rangle(0.5687)$

Table A.5. Excitation energies, E, and many-particle wave functions of excited states corresponding to the peaks in the linear absorption spectrum of B_6 – octahedron isomer (*cf.* Fig. 2(e)). The subscripts $\parallel$ and $\perp$, in the peak number denote the absorption due to light polarized in, and perpendicular to the plane of pyramidal base, respectively. The rest of the information is the same as given in the caption for Table A.1.

Peak	E (eV)	f_{12}	Wave Function
Reference			$\|H_1^1; H_2^1\rangle$
$I_{\parallel,\perp}$	3.63	0.0047	$\|H-1 \rightarrow L\rangle(0.8716)$ $\|H-1 \rightarrow L+1\rangle(0.8716)$ $\|H-2 \rightarrow L+1\rangle(0.2638)$ $\|H-2 \rightarrow L\rangle(0.2638)$
$II_{\parallel,\perp}$	5.56	0.0129	$\|H-1 \rightarrow L+1\rangle$ (0.5440) $\|H-1 \rightarrow L\rangle(0.5440)$ $\|H-1 \rightarrow L\rangle(0.5277)$ $\|H-1 \rightarrow L+1\rangle(0.5277)$
$III_{\parallel,\perp}$	6.05	0.0357	$\|H-1 \rightarrow L\rangle$ (0.6603) $\|H-1 \rightarrow L+1\rangle(0.6603)$ $\|H-1 \rightarrow L+1\rangle$ (0.4383) $\|H-1 \rightarrow L\rangle(0.4383)$
$IV_{\parallel,\perp}$	7.65	0.0149	$\|H-1 \rightarrow L\rangle(0.6741)$ $\|H-1 \rightarrow L+1\rangle(0.4383)$ $\|H-2 \rightarrow H_2\rangle(0.5346)$ $\|H-2 \rightarrow L+1\rangle(0.5346)$

Table A.6. Excitation energies, E, and many-particle wave functions of excited states corresponding to the peaks in the linear absorption spectrum of B_6 – threaded tetramer isomer (*cf.* Fig. 2(f)). The subscript x in the peak number denote the absorption due to light polarized along the long axis, and, y, z denotes polarization perpendicular to it. The rest of the information is the same as given in the caption for Table A.1.

Peak	E (eV)	f_{12}	Wave Function
Reference			$\|H_1^1; H_2^1\rangle$
I_x	2.74	0.1116	$\|H-1 \rightarrow H_2\rangle(0.5535)$ $\|H_1 \rightarrow L+9\rangle(0.3854)$
II_x	3.33	0.2917	$\|H-1 \rightarrow H_2\rangle(0.7564)$ $\|H_1 \rightarrow L+9\rangle(0.2492)$ $\|H_1 \rightarrow L+3\rangle(0.2465)$
III_z	3.90	0.0480	$\|H_1 \rightarrow L\rangle(0.8447)$ $\|H-1 \rightarrow L+9\rangle(0.2022)$
IV_z	4.33	0.1507	$\|H-1 \rightarrow L+9\rangle(0.4175)$ $\|H-1 \rightarrow L+3\rangle(0.4043)$
V_y	5.09	0.0338	$\|H-3 \rightarrow L+9\rangle(0.5013)$ $\|H-3 \rightarrow L+3\rangle(0.4697)$
VI_y	5.43	0.0852	$\|H-1 \rightarrow L+1\rangle(0.7137)$ $\|H-2 \rightarrow L\rangle(0.2694)$

Table A.7. Excitation energies, E, and many-particle wave functions of excited states corresponding to the peaks in the linear absorption spectrum of B_6 – threaded trimer isomer (*cf.* Fig. 2(g)). The subscript $\|$, in the peak number denotes the absorption due to light polarized along the long axis of the isomer. The rest of the information is the same as given in the caption for Table A.1.

Peak	E (eV)	f_{12}	Wave Function
Reference			$\|H_1^1; H_2^1\rangle$
$I_{\|}$	5.42	1.4376	$\|H-3 \rightarrow L\rangle(0.8262)$ $\|H-1 \rightarrow L+1\rangle(0.3212)$
$II_{\|}$	5.66	2.6846	$\|H-1 \rightarrow L+1\rangle(0.6710)$ $\|H-3 \rightarrow L\rangle(0.3680)$
$III_{\|}$	6.25	0.5077	$\|H-4 \rightarrow L+1\rangle(0.6263)$ $\|H-1 \rightarrow L+11\rangle(0.2702)$ $\|H-1 \rightarrow L+1\rangle(0.2701)$

Table A.8. Excitation energies, E, and many-particle wave functions of excited states corresponding to the peaks in the linear absorption spectrum of B_6 – twisted trimers isomer (*cf.* Fig. 2(h)). The subscripts $\parallel$ and $\perp$, in the peak number denote the absorption due to light polarized along, and perpendicular to the long axis of the isomer, respectively. The rest of the information is the same as given in the caption for Table A.3.

Peak	E (eV)	f_{12}	Wave Function
$I_{\parallel}$	1.02	0.0422	$\|H \rightarrow L\rangle(0.6550)$ $\|H-1 \rightarrow L\rangle(0.6550)$ $\|H \rightarrow L+1\rangle(0.5612)$ $\|H-1 \rightarrow L+1\rangle(0.5612)$
$II_{\perp}$	2.22	0.1279	$\|H-2 \rightarrow L\rangle(0.7650)$ $\|H-3 \rightarrow L+1\rangle(0.5316)$
$III_{\parallel}$	3.58	0.1870	$\|H-2 \rightarrow L+2\rangle(0.4374)$ $\|H-5 \rightarrow L\rangle(0.4374)$ $\|H-4 \rightarrow L\rangle(0.4371)$ $\|H-2 \rightarrow L+3\rangle(0.4371)$
$IV_{\parallel}$	4.72	0.4337	$\|H-2 \rightarrow L+2\rangle(0.4874)$ $\|H-2 \rightarrow L+3\rangle(0.4874)$ $\|H \rightarrow L+26\rangle(0.3268)$ $\|H-1 \rightarrow L+26\rangle(0.3268)$
$V_{\perp}$	5.26	0.3570	$\|H-5 \rightarrow L+3\rangle(0.5117)$ $\|H-4 \rightarrow L+2\rangle(0.5010)$
$VI_{\perp}$	5.87	3.4368	$\|H \rightarrow L+3\rangle(0.5962)$ $\|H-1 \rightarrow L+2\rangle(0.5962)$
$VII_{\parallel}$	6.39	0.2265	$\|H-3 \rightarrow L+2\rangle(0.4908)$ $\|H-3 \rightarrow L+3\rangle\ (0.4908)$ $\|H-2 \rightarrow L+3\rangle(0.4561)$ $\|H-2 \rightarrow L+2\rangle\ (0.4561)$
$VIII_{\perp}$	6.98	0.6645	$\|H-3 \rightarrow L+1\rangle(0.6479)$ $\|H-2 \rightarrow L\rangle(0.5508)$
$IX_{\parallel}$	7.25	0.3140	$\|H \rightarrow L+4\rangle\ (0.5209)$ $\|H-1 \rightarrow L+4\rangle\ (0.5209)$ $\|H \rightarrow L+7\rangle\ (0.4072)$ $\|H-1 \rightarrow L+7\rangle\ (0.4072)$

Table A.9. Excitation energies, E, and many-particle wave functions of excited states corresponding to the peaks in the linear absorption spectrum of B_6 – planar trimers isomer (*cf.* Fig. 2(i)). The subscripts $\parallel$ and $\perp$, in the peak number denote the absorption due to light polarized in, and perpendicular to the plane of the isomer, respectively. The rest of the information is the same as given in the caption for Table A.3.

Peak	E (eV)	f_{12}	Wave Function
$I_\perp$	0.97	0.0393	$\|H \rightarrow L\rangle$ (0.7804) $\|H-1 \rightarrow L+1\rangle$(0.5529)
$II_\parallel$	2.22	0.1261	$\|H-2 \rightarrow L\rangle$(0.7603) $\|H-4 \rightarrow L+1\rangle$(0.5634)
$III_\parallel$	3.57	0.1293	$\|H-2 \rightarrow L+2\rangle$ (0.6070) $\|H-3 \rightarrow L\rangle$(0.5440)
$IV_\parallel$	4.67	0.7257	$\|H-3 \rightarrow L+2\rangle$ (0.7242) $\|H \rightarrow L+12\rangle$ (0.3824) $\|H-2 \rightarrow L+2\rangle$ (0.5131) $\|H-3 \rightarrow L\rangle$ (0.4653)
$V_\parallel$	6.43	4.5721	$\|H \rightarrow L+12\rangle$(0.5256) $\|H-3 \rightarrow L+2\rangle$(0.4859)
$VI_\parallel$	6.99	1.8466	$\|H-4 \rightarrow L+1\rangle$(0.5794) $\|H \rightarrow L+7\rangle$(0.5156)
$VII_\parallel$	7.34	0.6386	$\|H \rightarrow L+12\rangle$(0.6754) $\|H \rightarrow L+7\rangle$(0.4922)

Table A.10. Excitation energies, E, and many-particle wave functions of excited states corresponding to the peaks in the linear absorption spectrum of B_6 – convex bowl isomer (*cf.* Fig. 2(j)). The subscripts $\parallel$ and $\perp$, in the peak number denote the absorption due to light polarized in, and perpendicular to the plane of the isomer, respectively. The rest of the information is the same as given in the caption for Table A.3.

Peak	E (eV)	f_{12}	Wave Function
$I_{\parallel}$	1.58	0.0486	$\|H-1\rightarrow L+1\rangle$ (0.9774)
$II_{\parallel,\perp}$	1.80	0.0679	$\|H\rightarrow L+2\rangle$(0.9079) $\|H-1\rightarrow L+3\rangle$(0.2748)
$III_{\parallel}$	2.43	0.6023	$\|H\rightarrow L\rangle$ (0.8644) $\|H-4\rightarrow L+1\rangle$(0.4364)
$IV_{\parallel}$	2.89	0.1811	$\|H-1\rightarrow L\rangle$ (0.8058) $\|H-3\rightarrow L+1\rangle$ (0.5421)
$V_{\parallel}$	4.09	0.1602	$\|H-4\rightarrow L\rangle$(0.5608) $\|H-3\rightarrow L+1\rangle$(0.5347)
$VI_{\parallel,\perp}$	5.13	0.0649	$\|H-4\rightarrow L+3\rangle$(0.9070) $\|H-3\rightarrow L+2\rangle$(0.1753)
$VII_{\parallel}$	6.21	1.4363	$\|H\rightarrow L+7\rangle$(0.4118) $\|H\rightarrow L+4\rangle$(0.3622)
$VIII_{\perp}$	6.39	2.2019	$\|H\rightarrow L+6\rangle$(0.4335) $\|H-2\rightarrow L+3\rangle$(0.4081)
$IX_{\parallel}$	6.90	0.1476	$\|H\rightarrow L+8\rangle$(0.4435) $\|H\rightarrow L+13\rangle$(0.3534)

Table A.11. Excitation energies, E, and many-particle wave functions of excited states corresponding to the peaks in the linear absorption spectrum of B_6 – linear isomer (*cf.* Fig. 2(k)). The subscripts $\parallel$ and $\perp$, in the peak number denote the absorption due to light polarized along, and perpendicular to the axis of the isomer, respectively. The rest of the information is the same as given in the caption for Table A.3.

Peak	E (eV)	f_{12}	Wave Function
$I_{\parallel}$	5.51	12.8358	$\|H-1\rightarrow L+3\rangle$(0.6510) $\|H\rightarrow L+2\rangle$(0.6489)
$II_{\perp}$	6.51	1.6532	$\|H\rightarrow L+4\rangle$(0.7148) $\|H-1\rightarrow L+4\rangle$(0.7148) $\|H-3\rightarrow L+8\rangle$(0.3847) $\|H-2\rightarrow L+8\rangle$(0.3847)

Table A.12. Excitation energies, E, and many-particle wave functions of excited states corresponding to the peaks in the linear absorption spectrum of B_6^+ – planar ring isomer (*cf.* Fig. 4(a)). The subscripts $\parallel$ and $\perp$, in the peak number denote the absorption due to light polarized in, and perpendicular to the plane of the isomer, respectively. In the wave function, the bracketed numbers are the CI coefficients of a given electronic configuration. Symbols H, H_1 and L denote HOMO, SOMO and LUMO orbitals respectively.

Peak	E (eV)	f_{12}	Wave Function
Reference			$\|H_1^1\rangle$
$I_\perp$	0.63	0.0075	$\|H_1 \rightarrow L\rangle(0.9667)$ $\|H-2 \rightarrow L+16\rangle(0.1229)$
$II_\parallel$	4.43	0.9637	$\|H-1 \rightarrow L\rangle(0.7448)$ $\|H_1 \rightarrow L+10\rangle(0.4227)$
$III_\parallel$	5.18	0.0565	$\|H-2 \rightarrow L+1\rangle(0.6283)$ $\|H-1 \rightarrow L+1\rangle(0.5264)$
$IV_\parallel$	5.64	0.4310	$\|H-1 \rightarrow L+2\rangle(0.6350)$ $\|H-3 \rightarrow L+3\rangle(0.5173)$
$V_\parallel$	6.06	0.1576	$\|H-3 \rightarrow L+3\rangle(0.5624)$ $\|H-1 \rightarrow L+3\rangle(0.4278)$

Table A.13. Excitation energies, E, and many-particle wave functions of excited states corresponding to the peaks in the linear absorption spectrum of B_6^+ – bulged wheel isomer (*cf.* Fig. 4(b)). The subscripts $\parallel$ and $\perp$, in the peak number denote the absorption due to light polarized in, and perpendicular to the plane of the wheel, respectively. The rest of the information is the same as given in the caption for Table A.12.

Peak	E (eV)	f_{12}	Wave Function
Reference			$\|H_1^1\rangle$
$I_\parallel$	1.67	0.0159	$\|H-2\rightarrow H_1\rangle(0.9568)$ $\|H_1\rightarrow L+3\rangle(0.1270)$
$II_\parallel$	3.25	0.0061	$\|H_1\rightarrow L\rangle(0.5877)$ $\|H_1\rightarrow L+3\rangle(0.3945)$
$III_\parallel$	3.65	0.0021	$\|H_1\rightarrow L+2\rangle(0.8106)$ $\|H_1\rightarrow L+1\rangle(0.2830)$
$IV_\parallel$	4.20	0.0998	$\|H-1\rightarrow L\rangle(0.5760)$ $\|H-2\rightarrow L\rangle(0.5743)$
$V_\parallel$	4.46	0.0312	$\|H-1\rightarrow L+2\rangle(0.7945)$ $\|H_1\rightarrow L\rangle(0.2711)$
$VI_\parallel$	4.69	0.0417	$\|H-1\rightarrow L+2\rangle(0.7945)$ $\|H-2\rightarrow L\rangle(0.2711)$
$VII_\parallel$	4.91	0.0453	$\|H-2\rightarrow L+1\rangle(0.6517)$ $\|H-1\rightarrow L+1\rangle(0.4364)$
$VIII_\parallel$	5.60	0.4219	$\|H-1\rightarrow L+3\rangle(0.6402)$ $\|H-2\rightarrow L\rangle(0.4002)$
$IX_{\parallel,\perp}$	5.77	0.2700	$\|H-2\rightarrow L+2\rangle(0.8807)$ $\|H-1\rightarrow L+4\rangle(0.6632)$ $\|H-2\rightarrow L+1\rangle(0.3734)$ $\|H-2\rightarrow L\rangle(0.2952)$
$X_\parallel$	6.00	0.5544	$\|H-3\rightarrow L\rangle(0.4788)$ $\|H-2\rightarrow L+1\rangle(0.4263)$
$XI_\parallel$	6.27	0.3573	$\|H-2\rightarrow L+3\rangle(0.6862)$ $\|H-4\rightarrow L\rangle(0.4386)$

Table A.14. Excitation energies, E, and many-particle wave functions of excited states corresponding to the peaks in the linear absorption spectrum of B_6^+ – planar ring (II) isomer (*cf.* Fig. 4(c)). The subscript $\parallel$ in the peak number denote the absorption due to light polarized in the plane of the isomer. The rest of the information is the same as given in the caption for Table A.12.

Peak	E (eV)	f_{12}	Wave Function
Reference			$\|H_1^1\rangle$
$I_\parallel$	1.18	0.0182	$\|H-1\rightarrow L\rangle(0.6957)$ $\|H-2\rightarrow H_1\rangle(0.6943)$
$II_\parallel$	3.47	1.5345	$\|H-1\rightarrow L\rangle(0.7424)$ $\|H-2\rightarrow H_1\rangle(0.4272)$
$III_\parallel$	4.70	0.1042	$\|H-2\rightarrow L+1\rangle(0.7037)$ $\|H-4\rightarrow L\rangle(0.4979)$
$IV_\parallel$	4.93	0.1114	$\|H-1\rightarrow L+3\rangle(0.9077)$ $\|H-5\rightarrow L\rangle(0.1606)$
$V_\parallel$	5.12	0.0673	$\|H-4\rightarrow L\rangle(0.7687)$ $\|H-3\rightarrow L+2\rangle(0.5208)$
$VI_\parallel$	6.43	0.8286	$\|H_1\rightarrow L+6\rangle(0.6655)$ $\|H-1\rightarrow L+3\rangle(0.4625)$

Table A.15. Excitation energies, E, and many-particle wave functions of excited states corresponding to the peaks in the linear absorption spectrum of B_6^+ – incomplete wheel (quartet) isomer (*cf.* Fig. 4(d)). The subscripts $\parallel$ and $\perp$, in the peak number denote the absorption due to light polarized in, and perpendicular to the plane of the isomer, respectively. In the wave function, the bracketed numbers are the CI coefficients of a given electronic configuration. Symbols H, H_1, H_2, H_3 and L denote HOMO, SOMOs and LUMO orbitals respectively.

Peak	E (eV)	f_{12}	Wave Function
Reference			$\|H_1^1;H_2^1;H_3^1\rangle$
$I_\perp$	2.94	0.0608	$\|H_1\rightarrow L+1\rangle(0.7513)$ $\|H_2\rightarrow L\rangle(0.6261)$
$II_\parallel$	3.25	0.1207	$\|H-5\rightarrow H_3\rangle(0.7994)$ $\|H-4\rightarrow L\rangle(0.3377)$
$III_\perp$	4.84	0.0248	$\|H_3\rightarrow L\rangle(0.8592)$ $\|H_1\rightarrow L+1\rangle(0.2632)$
$IV_\parallel$	5.60	0.0552	$\|H-3\rightarrow H_2\rangle(0.6397)$ $\|H_1\rightarrow L+3\rangle(0.4131)$
$V_\parallel$	6.8	0.0674	$\|H-3\rightarrow H_1\rangle(0.6876)$ $\|H-4\rightarrow L\rangle(0.4045)$
$VI_\parallel$	7.25	0.1363	$\|H-5\rightarrow H_2\rangle(0.7232)$ $\|H_2\rightarrow L\rangle(0.2883)$
$VII_\perp$	7.39	0.0336	$\|H-3\rightarrow L\rangle(0.4522)$ $\|H_1\rightarrow L+5\rangle(0.3485)$

Table A.16. Excitation energies, E, and many-particle wave functions of excited states corresponding to the peaks in the linear absorption spectrum of B_6^+ – threaded trimer (quartet) isomer (*cf.* Fig. 4(e)). The subscripts $\parallel$ and $\perp$, in the peak number denote the absorption due to light polarized along, and perpendicular to the long axis of the isomer, respectively. The rest of the information is the same as given in the caption for Table A.15.

Peak	E (eV)	f_{12}	Wave Function
Reference			$\|H_1^1; H_2^1; H_3^1\rangle$
$I_{\parallel}$	3.18	0.4369	$\|H-3 \rightarrow H_3\rangle(0.6993)$ $\|H-3 \rightarrow L\rangle(0.5802)$
$II_{\parallel,\perp}$	4.48	0.1117	$\|H_3 \rightarrow L+2\rangle(0.8855)$ $\|H-3 \rightarrow L\rangle(0.7012)$ $\|H-4 \rightarrow L+2\rangle(0.4816)$ $\|H-3 \rightarrow L+3\rangle(0.3931)$
$III_{\parallel}$	5.03	2.3151	$\|H_3 \rightarrow L\rangle(0.6337)$ $\|H_2 \rightarrow L+1\rangle(0.5640)$

Table A.17. Excitation energies, E, and many-particle wave functions of excited states corresponding to the peaks in the linear absorption spectrum of B_6^+ – tetragonal bipyramid isomer (*cf.* Fig. 4(f)). The subscripts $\parallel$ and $\perp$, in the peak number denote the absorption due to light polarized in, and perpendicular to the square plane of bipyramid, respectively. The rest of the information is the same as given in the caption for Table A.12.

Peak	E (eV)	f_{12}	Wave Function
Reference			$\|H_1^1\rangle$
$I_{\perp}$	1.58	0.2525	$\|H_1 \rightarrow L+2\rangle(0.7189)$ $\|H-1 \rightarrow L+2\rangle(0.6154)$
$II_{\parallel}$	1.97	0.0803	$\|H_1 \rightarrow L+1\rangle(0.7492)$ $\|H-1 \rightarrow L+1\rangle(0.5593)$
$III_{\parallel,\perp}$	3.87	0.0272	$\|H-2 \rightarrow L\rangle(0.8717)$ $\|H-1 \rightarrow L\rangle(0.8684)$ $\|H-2 \rightarrow L+1\rangle(0.4082)$ $\|H_1 \rightarrow L\rangle(0.3497)$
$IV_{\parallel}$	4.36	0.0287	$\|H-2 \rightarrow L+2\rangle(0.8419)$ $\|H-1 \rightarrow L\rangle(0.3385)$
$V_{\parallel}$	4.55	0.0440	$\|H-2 \rightarrow L+2\rangle(0.9001)$ $\|H-4 \rightarrow L+2\rangle(0.8807)$ $\|H-1 \rightarrow L\rangle(0.2555)$ $\|H-5 \rightarrow L\rangle(0.1997)$
$VI_{\parallel,\perp}$	5.04	0.8028	$\|H-4 \rightarrow L+2\rangle(0.8991)$ $\|H-1 \rightarrow L+2\rangle(0.6152)$ $\|H-4 \rightarrow L+3\rangle(0.5964)$ $\|H-1 \rightarrow L\rangle(0.5334)$ $\|H-2 \rightarrow L+2\rangle(0.4299)$ $\|H-1 \rightarrow L+3\rangle(0.3269)$

Table A.18. Excitation energies, E, and many-particle wave functions of excited states corresponding to the peaks in the linear absorption spectrum of B_6^+ – linear (quartet) isomer (*cf.* Fig. 4(g)). The subscripts $\parallel$ and $\perp$, in the peak number denote the absorption due to light polarized along, and perpendicular to the long axis of the isomer, respectively. The rest of the information is the same as given in the caption for Table A.15.

Peak	E (eV)	f_{12}	Wave Function
Reference			$\|H_1^1; H_2^1; H_3^1\rangle$
$I_\parallel$	0.93	0.1533	$\|H-3 \rightarrow H_3\rangle(0.8624)$ $\|H_2 \rightarrow L\rangle(0.3187)$
$II_\perp$	3.62	0.0677	$\|H_2 \rightarrow L\rangle(0.7478)$ $\|H_1 \rightarrow L\rangle(0.6474)$
$III_\parallel$	5.02	0.6861	$\|H-3 \rightarrow L+4\rangle(0.9263)$ $\|H-3 \rightarrow L+12\rangle(0.2264)$
$IV_\parallel$	5.60	9.8432	$\|H-4 \rightarrow L\rangle(0.6486)$ $\|H-3 \rightarrow L+4\rangle(0.3521)$

Table A.19. Excitation energies, E, and many-particle wave functions of excited states corresponding to the peaks in the linear absorption spectrum of B_6^+ – planar trimers isomer (*cf.* Fig. 4(h)). The subscripts $\parallel$ and $\perp$, in the peak number denote the absorption due to light polarized in, and perpendicular to the plane of the isomer, respectively. The rest of the information is the same as given in the caption for Table A.12.

Peak	E (eV)	f_{12}	Wave Function
Reference			$\|H_1^1\rangle$
$I_\parallel$	0.77	0.2915	$\|H-2 \rightarrow H_1\rangle(0.9647)$ $\|H_1 \rightarrow L+4\rangle(0.1605)$
$II_\perp$	1.33	0.0108	$\|H_1 \rightarrow L\rangle(0.8340)$ $\|H-2 \rightarrow L+1\rangle(0.5093)$
$III_\perp$	2.08	0.0378	$\|H-2 \rightarrow L+1\rangle(0.9744)$ $\|H_1 \rightarrow L\rangle(0.1888)$
$IV_\perp$	2.51	0.0103	$\|H-3 \rightarrow H_1\rangle(0.9414)$ $\|H-1 \rightarrow L+4\rangle(0.2905)$
$V_\parallel$	2.86	0.1131	$\|H-1 \rightarrow L\rangle(0.7701)$ $\|H-3 \rightarrow L+1\rangle(0.5892)$
$VI_\parallel$	4.16	0.1267	$\|H-1 \rightarrow L+2\rangle(0.6627)$ $\|H-4 \rightarrow L\rangle(0.5105)$
$VII_\parallel$	5.30	0.4383	$\|H_1 \rightarrow L+9\rangle(0.5023)$ $\|H-1 \rightarrow L+2\rangle(0.4505)$

References

1. J.A. Alonso, *Structure and Properties of Atomic Nanostructures* (Imperial College Press, London, 2005)
2. P. Jena, S. Khanna, B. Rao, eds., *Physics and Chemistry of Small Clusters* (Plenum, New York, 1987)
3. I. Cabria, M.J. López, J.A. Alonso, Nanotechnology **17**, 778 (2006)
4. H.J. Zhai, B. Kiran, J. Li, L.S. Wang, Nature Materials **2**, 827 (2003)
5. J. Jimenez-Halla, R. Islas, T. Heine, G. Merino, Ang. Chem. Int. Ed. **49**, 5668 (2010)
6. W. Huang, A.P. Sergeeva, H.J. Zhai, B.B. Averkiev, L.S. Wang, A.I. Boldyrev, Nat. Chem. **2**, 202 (2010)
7. A.N. Alexandrova, A.I. Boldyrev, H.J. Zhai, L.S. Wang, Coord. Chem. Rev. **250**, 2811 (2006)
8. A.N. Alexandrova, H.J. Zhai, L.S. Wang, A.I. Boldyrev, Inorg. Chem. **43**, 3552 (2004)
9. B. Kiran, S. Bulusu, H.J. Zhai, S. Yoo, X.C. Zeng, L.S. Wang, Proc. Nat. Acad. Sci. USA **102**, 961 (2005)
10. H.J. Zhai, A.N. Alexandrova, K.A. Birch, A.I. Boldyrev, L.S. Wang, Angew. Chem. Int. Ed. **42**, 6004 (2003)
11. C. Romanescu, T.R. Galeev, W.L. Li, A.I. Boldyrev, L.S. Wang, Angew. Chem. Int. Ed. **50**, 9334 (2011)
12. A.N. Alexandrova, A.I. Boldyrev, H.J. Zhai, L.S. Wang, E. Steiner, P.W. Fowler, J. Phys. Chem. A **107**, 1359 (2003)
13. S.J.L. Placa, P.A. Roland, J.J. Wynne, Chem. Phys. Lett. **190**, 163 (1992)
14. L. Hanley, J.L. Whitten, S.L. Anderson, J. Phys. Chem. **92**, 5803 (1988)
15. I. Boustani, Phys. Rev. B **55**, 16426 (1997)
16. M. Atiş, C. Özdogan, Z.B. Güvenç, Int. J. Quantum Chem. **107**, 729 (2007)
17. S. Botti, A. Castro, N.N. Lathiotakis, X. Andrade, M.A.L. Marques, Phys. Chem. Chem. Phys. **11**, 4523 (2009)
18. R. Shinde, A. Shukla, Nano LIFE **2**, 1240004 (2012)
19. S. Tirapattur, M. Bellette, M. Leclerc, G. Durocher, J. Mol. Struct. THEO. **625**, 141 (2003)
20. J.B. Lagowski, J. Mol. Struct. THEO. **589–590**, 125 (2002)
21. T.A. Dahlseid, M.M. Kappes, J.A. Pople, M.A. Ratner, J. Chem. Phys. **96**, 4924 (1992)
22. J. Cornil, D. Beljonne, R. Friend, J. Brédas, Chem. Phys. Lett. **223**, 82 (1994)
23. L. Mitas, J. Therrien, R. Twesten, G. Belomoin, M.H. Nayfeh, Appl. Phys. Lett. **78**, 1918 (2001)
24. K. Harigaya, S. Abe, Phys. Rev. B **49**, 16746 (1994)
25. V. Bonačić-Koutecký, J. Gaus, M.F. Guest, J. Koutecký, J. Chem. Phys. **96**, 4934 (1992)
26. M.J. Frisch, G.W. Trucks, H.B. Schlegel, G.E. Scuseria, M.A. Robb, J.R. Cheeseman, G. Scalmani, V. Barone, B. Mennucci, G.A. Petersson et al., *Gaussian 09 Revision A.02*, Gaussian Inc. Wallingford CT 2009
27. L.E. McMurchie, S.T. Elbert, S.R. Langhoff, E.R. Davidson, MELD package from Indiana University. It has been modified by us to handle bigger systems.
28. K.L. Schuchardt, B.T. Didier, T. Elsethagen, L. Sun, V. Gurumoorthi, J. Chase, J. Li, T.L. Windus, J. Chem. Inf. Model. **47**, 1045 (2007)
29. D. Feller, J. Comput. Chem. **17**, 1571 (1996)
30. A. Allouche, J. Comput. Chem. **32**, 174 (2011)
31. G. Wei, Z. Pu, R. Zou, G. Li, Q. Luo, Sci. China Chem. **53**, 202 (2010)
32. V. Bonačić-Koutecký, P. Fantucci, J. Koutecký, Chem. Rev. **91**, 1035 (1991)
33. J. Blanc, V.B. Koutecký, M. Broyer, J. Chevaleyre, P. Dugourd, J. Koutecký, C. Scheuch, J.P. Wolf, L. Wöste, J. Chem. Phys. **96**, 1793 (1992)
34. J. Ma, Z. Li, K. Fan, M. Zhou, Chem. Phys. Lett. **372**, 708 (2003)
35. R. Shinde, A. Shukla (2012), in preparation